Inorganic Chemistry
Article

Inorg. Chem. **2010**, *49*, 8487–8494 **8487**
DOI: 10.1021/ic101060s

All-Nitrogen Coordinated Amidinato/Imido Complexes of Molybdenum and Tungsten: Syntheses and Characterization

Vanessa Gwildies, Tobias B. Thiede, Saeed Amirjalayer, Louay Alsamman, Anjana Devi, and Roland A. Fischer*

Lehrstuhl für Anorganische Chemie II, Ruhr-Universität Bochum, Universitätsstrasse 150, 44801 Bochum, Germany

Received May 25, 2010

The first all-nitrogen coordinated bis(alkylamidinato)/bis(alkylimido) complexes of molybdenum and tungsten, $[Mo(NtBu)_2\{(iPrN)_2CMe\}_2]$and $[W(NtBu)_2\{(iPrN)_2CMe\}_2]$, have been synthesized and fully characterized by ^1H and ^{13}C NMR spectroscopy, elemental analyses, high-resolution electron impact mass spectrometry, and Fourier transform infrared spectroscopy. Density functional theory calculations of the tungsten complex allow for geometry optimization and structural characterization by assignment of the NMR data, in particular a comparison of the experimental ^{13}C NMR signals with the calculated ones. Both compounds sublime without decomposition at 130 °C and 1 mTorr and show rapid decomposition above 250 °C, hence representing promising vapor-phase deposition routes for metal nitride based thin-film materials.

Introduction

The importance of molybdenum and tungsten nitride based materials originates from a range of properties, e.g., their ability to act as diffusion barriers in microelectronic devices, their chemical inertness, and their refractive properties, which are useful as hard and protective coatings.[1] Metal−organic chemical vapor deposition (MOCVD) and related techniques such as atomic layer deposition (ALD) have been proven as versatile techniques for the fabrication of various kinds of thin films; hence, the availability of a suitable precursor has to be assured. For such applications, all-nitrogen coordinated molybdenum and tungsten precursors exhibiting the appropriate thermal properties, i.e., volatility and clean decomposition, are preferred and the still quite limited range of available precursors of this kind has been reviewed, recently.[1] Alkylimido ligands play a crucial role for this precursor concept because they can act as "spectator" or "ancillary" ligands.[2] Coming from the widely used precursor molecule $[Mo(NtBu)_2Cl_2(dme)]$[3], its solvent-free congener $[Mo(NtBu)_2Cl_2]$[4] and the related tungsten compound $[WCl_2(NtBu)_2py_2]$,[5] a couple of interesting molecules containing bis(*tert*-butylimido) groups have been synthesized.[6] Apart from their "spectator-like" behavior, *tert*-butylimido ligands of $[Mo(NtBu)_2Cl_2(dme)]$ also take part in substitution processes, e.g., by reaction with an amine,[7] or undergo imide/imine metathesis.[8] $[Mo(NtBu)_2Cl_2(dme)]$ and $[Mo(O)_2Cl_2(dme)]$ exchange their oxo and imido ligands to form $[Mo(O)(NtBu)Cl_2(dme)]$,[9] a versatile compound permitting access to unique structural features[10] and catalytic oxidation chemistry.[11] In contrast, the intermetal exchange of imido ligands has been found to be unsuccessful.[9] Additionally, reagents like diphenylphosphinoaniline[12] and *tert*-butylsilanol/HCl[13] cause a loss of one imido group, affording (in the latter case by Na/Hg reduction) a mercury complex with an unusual three-center, four-electron bonding situation.[14]

*To whom correspondence should be addressed. E-mail: roland.fischer@rub.de.

(1) Fischer, R. A.; Parala, H. In *Chemical Vapor Deposition: Precursors, Processes and Applications*; Jones, A. C., Hitchman, M. L., Eds.; RSC: Cambridge, U.K., 2009; Chapter 9.
(2) Gade, L. H.; Mountford, P. *Coord. Chem. Rev.* **2001**, *216*−*217*, 65–97.
(3) Dyer, P. W.; Gibson, V. C.; Howard, J. A. K.; Whittle, B.; Wilson, C. *J. Chem. Soc., Chem. Commun.* **1992**, *22*, 1666–1668.
(4) Schoettel, G.; Kress, J.; Osborn, J. A. *J. Chem. Soc., Chem. Commun.* **1989**, *15*, 1062–1063.
(5) Rische, D.; Baunemann, A.; Winter, M.; Fischer, R. A. *Inorg. Chem.* **2006**, *45*, 269–277.
(6) (a) Lyashenko, G.; Herbst-Irmer, R.; Jancik, V.; Pal, A.; Mösch-Zanetti, N. C. *Inorg. Chem.* **2008**, *47*, 113–120. (b) Radius, U.; Sundermeyer, J.; Peters, K.; von Schnering, H. G. *Z. Anorg. Allg. Chem.* **2002**, *628*, 1226–1235. (c) Lavoie, N.; Ong, T.-G.; Gorelsky, S. I.; Korobkov, I.; Yap, G. P. A.; Richeson, D. S. *Organometallics* **2007**, *26*, 6586–6590.
(7) Bell, A.; Clegg, W.; Dyer, P. W.; Elsegood, M. R. J.; Gibson, V. C.; Marshall, E. L. *J. Chem. Soc., Chem. Commun.* **1994**, *22*, 2547–2548.
(8) Cantrell, G. K.; Meyer, T. Y. *Chem. Commun.* **1997**, *16*, 1551–1552.
(9) Gibson, V. C.; Graham, A. J.; Jolly, M.; Mitchell, J. P. *Dalton Trans.* **2003**, 4457–4465.
(10) Merkoulov, A.; Harms, K.; Sundermeyer, J. *Eur. J. Inorg. Chem.* **2005**, 4902–4906.
(11) Ramnauth, R.; Al-Juaid, S.; Motevalli, M.; Parkin, B. C.; Sullivan, A. C. *Inorg. Chem.* **2004**, *43*, 4072–4079.
(12) Redshaw, C.; Gibson, V. C.; Elsegood, M. R. J.; Clegg, W. *Chem. Commun.* **2007**, 1951–1953.
(13) Rosenfeld, D. C.; Wolczanski, P. T.; Barakat, K. A.; Buda, C.; Cundari, T. R.; Schroeder, F. C.; Lobkovsky, E. B. *Inorg. Chem.* **2007**, *46*, 9715–9735.
(14) Rosenfeld, D. C.; Wolczanski, P. T.; Barakat, K. A.; Buda, C.; Cundari, T. R. *J. Am. Chem. Soc.* **2005**, *127*, 8262–8263.

Published on Web 08/16/2010

More recently, some hetereoleptic all-nitrogen coordinated molybdenum and tungsten complexes featuring alkylimido/alkylguanidinato ligand combinations[15] proved to be quite useful precursors for application in MOCVD[15b] and ALD.[15e] However, all-nitrogen coordinated bis(amidinato) and bis(imido) complexes of the type $[M(RN)_2\{(R'N)_2CR''\}_2]$ have not been reported yet. Amidinato ligands $[(R'N)_2CR'']^-$ are closely related congeners to guanidinato ligands $[(R'N)_2C(NR''_2)]^-$, and we were thus led to investigate the possibility of deriving the respective bis(amidinato)/bis(imido) complexes $[M(NtBu)_2\{(R'N)_2CR''\}_2]$ (M = Mo, W). The so-far-known coordination chemistry of amidinato ligands of these metals demonstrates structurally interesting features like a rare η^1-coordination mode of the amidinato ligand,[16] a bicyclic tungsten amidinato complex,[17] and a chiral complex with the Mo atom as an asymmetric center.[18] Interestingly, the first characterized metallaamidinato complex was with molybdenum,[19] and encumbering amidinato ligands were used for stabilization of the Mo−Mo quintuple bond, the shortest metal−metal bond beyond the first-row transition metals.[20] A couple of dimolybdenum and ditungsten amidinato compounds reveal a "paddlewheel" structure and should be mentioned here as well.[21] In particular, amidinato-chloroimido complexes of molybdenum and tungsten have already been published.[22] Our effort was to avoid halogen substituents because of the possible corrosive nature of hydrohalogens during MOCVD or ALD, which can etch substrates and may incorporate into the deposited films. Herein, we report in detail on the synthesis and characterization of the two representative compounds $[Mo(NtBu)_2\{(iPrN)_2CMe\}_2]$ (**1**) and $[W(NtBu)_2\{(iPrN)_2CMe\}_2]$ (**2**) as a part of our systematic study to combine the versatile characteristics of imido and amidinato ligands in order to achieve a further tunable all-nitrogen coordinated metal CVD precursor for tungsten and molybdenum nitride based thin films.

Experimental Section

General Procedures. All reactions and manipulations of air- and moisture-sensitive compounds were performed employing a conventional vacuum/argon line using standard Schlenk techniques. A sample preparation for further analysis was carried out in an argon-filled glovebox. All solvents were dried and purified by an MBraun solvent purification system and stored over molecular sieves (4 Å). The NMR solvents were degassed and dried over activated molecular sieves. The starting compounds, namely, methyllithium in diethyl ether (1.6M) (Acros) and *N*,*N*′-diisopropylcarbodiimide (Acros), were used as received. $[Mo(NtBu)_2Cl_2(dme)]$ and $[WCl_2(NtBu)_2py_2]$ were prepared according to literature-reported procedures.[3,5]

Table 1. Obtained Elemental Compositions of Complexes **1** and **2** by High-Resolution Mass Spectrometry

experimentally determined accurate mass	calculated exact mass	deviation in mmu	most likely corresponding elemental composition
522.330 261	522.330 751	0.5	$MoC_{24}H_{52}N_6$
608.376 709	608.376 299	−0.4	$WC_{24}H_{52}N_6$

Elemental Analysis. Elemental analyses were performed by using a CHSNO Vario EL instrument. Because of the possibility of carbide formation, the measured carbon values may deviate a little more from the calculated value as usual.

Physical Measurements. ^{1}H and ^{13}C NMR spectra were recorded on a Bruker Advance DRX 250. Electon ionization mass spectrometry (EI-MS) spectra were recorded using a Varian MAT spectrometer (R = 7000 for the high-resolution mass spectra; see Table 1). IR spectra were recorded on a Bruker Alpha Fourier transform infrared (FTIR) spectrometer and UV/vis spectra on a Perkin-Elmer Lamda 9 spectrometer. Thermal analysis data were obtained using a Seiko TG/DTA 6300S11 in a dinitrogen atmosphere (flow rate of 300 mL/min, ambient pressure, heating rate of 5 °C/min, sample weight of approximately 10 mg).

Quantum Chemical Calculations. *Ab initio* calculations, in particular density functional theory (DFT) methods, were carried out to investigate the structure of the tungsten complex and to verify the experimental data. All calculations were done using the *Gaussian 03* program package.[23] The full structure was optimized on the B-LYP[24] level with the Stuttgart effective relativistic small-core potential[25] for tungsten and the 6-31G basis set for carbon, nitrogen, and hydrogen. NMR shielding was calculated using the GIAO method as implemented in the *Gaussian 03* code. Tetramethylsilane was used as the reference for ^{13}C NMR. To analyze *cis*/*trans* isomers, a simple model of the complex was used and optimized with the same basis sets on the B3-LYP[24a,b,26] level.

MOCVD Experiments. A custom-built horizontal cold-wall MOCVD reactor operating under reduced pressure and equipped with a resistive heating system was used for thin-film growth. Initially, the reactor was pumped down to a base

(15) (a) Ward, B. D.; Dubberley, S. R.; Gade, L. H.; Mountford, P. *Inorg. Chem.* **2003**, *42*, 4961–4969. (b) Rische, D.; Parala, H.; Gemel, E.; Winter, M.; Fischer, R. A. *Chem. Mater.* **2006**, *18*, 6075–6082. (c) Rische, D.; Baunemann, A.; Winter, M.; Fischer, R. A. *Inorg. Chem.* **2006**, *45*, 269–277. (d) Gaess, D.; Harms, K.; Pokoj, M.; Stolz, W.; Sundermeyer, J. *Inorg. Chem.* **2007**, *46*, 6688–6701. (e) El-Kadri, O. M.; Heeg, M. J.; Winter, C. H. *Dalton Trans.* **2006**, 1943–1953.

(16) Yamaguchi, Y.; Ogata, K.; Kobayashi, K.; Ito, T. *Dalton Trans.* **2004**, 3982–3990.

(17) Legzdins, P.; Lumb, S. A.; Young, V. G. *Organometallics* **1998**, *17*, 854–871.

(18) Brunner, H.; Lukassek, J.; Agrifoglio, G. *J. Organomet. Chem.* **1980**, *195*, 63–76.

(19) Brunner, H.; Meier, W.; Wachter, J.; Bernal, I.; Raabe, E. *J. Organomet. Chem.* **1989**, *362*, 95–103.

(20) Tsai, Y.-C.; Chen, H.-Z.; Chang, C.-C.; Yu, J.-S. K.; Lee, G.-H.; Wang, Y.; Kuo, T.-S. *J. Am. Chem. Soc.* **2009**, *131*, 12534–12535.

(21) (a) Cotton, F. A.; Inglis, T.; Kilner, M.; Webb, T. R. *Inorg. Chem.* **1975**, *14*, 2023–2026. (b) Zinn, A.; Weller, F.; Dehnicke, K. *Z. Anorg. Allg. Chem.* **1991**, *594*, 106–112. (c) Brown, D. J.; Chisholm, M. H.; Gallucci, J. C. *Dalton Trans.* **2008**, 1615–1624.

(22) (a) Hao, H.; Cui, C.; Bai, G.; Roesky, H. W.; Noltemeyer, M.; Schmidt, H.-G.; Ding, Y. *Z. Anorg. Allg. Chem.* **2000**, *626*, 1660–1664. (b) Wilder, C. B.; Reitfort, L. L.; Abboud, K. A.; McElwee-White, L. *Inorg. Chem.* **2006**, *45*, 263–268.

(23) Frisch, M. J.; Trucks, G. W.; Schlegel, H. B.; Scuseria, G. E.; Robb, M. A.; Cheeseman, J. R.; Montgomery, J. A., Jr.; Vreven, T.; Kudin, K. N.; Burant, J. C.; Millam, J. M.; Iyengar, S. S.; Tomasi, J.; Barone, V.; Mennucci, B.; Cossi, M.; Scalmani, G.; Rega, N.; Petersson, G. A.; Nakatsuji, H.; Hada, M.; Ehara, M.; Toyota, K.; Fukuda, R.; Hasegawa, J.; Ishida, M.; Nakajima, T.; Honda, Y.; Kitao, O.; Nakai, H.; Klene, M.; Li, X.; Knox, J. E.; Hratchian, H. P.; Cross, J. B.; Adamo, C.; Jaramillo, J.; Gomperts, R.; Stratmann, R. E.; Yazyev, O.; Austin, A. J.; Cammi, R.; Pomelli, C.; Ochterski, J. W.; Ayala, P. Y.; Morokuma, K.; Voth, G. A.; Salvador, P.; Dannenberg, J. J.; Zakrzewski, V. G.; Dapprich, S.; Daniels, A. D.; Strain, M. C.; Farkas, O.; Malick, D. K.; Rabuck, A. D.; Raghavachari, K.; Foresman, J. B.; Ortiz, J. V.; Cui, Q.; Baboul, A. G.; Clifford, S.;Cioslowski, J.;Stefanov, B. B.;Liu, G.; Liashenko, A.; Piskorz, P.; Komaromi, I.; Martin, R. L.; Fox, D. J.; Keith, T.; Al-Laham, M. A.;Peng, C. Y.; Nanayakkara, A.; Challacombe, M.; Gill, P. M. W.; Johnson, B.; Chen, W.; Wong, M. W.; Gonzalez, C.; Pople, J. A. *Gaussian 03*, revision B.04; Gaussian: Pittsburgh, PA, 2003.

(24) (a) Becke, A. D. *Phys. Rev. A* **1988**, *38*, 3098–3100. (b) Lee, C.; Yang, W.; Parr, R. G. *Phys. Rev. B* **1988**, *37*, 785–789. (c) Miehlich, B.; Savin, A.; Stoll, H.; Preuss, H. *Chem. Phys. Lett.* **1989**, *157*, 200–206.

(25) Dolg, M.; Wedig, U.; Stoll, H.; Preuss, H. *J. Chem. Phys.* **1987**, *86*, 866–872.

(26) Becke, A. D. *J. Chem. Phys.* **1993**, *98*, 5648–5652.

Scheme 1. Syntheses of the Amidinato/Imido Complexes **1** and **2**

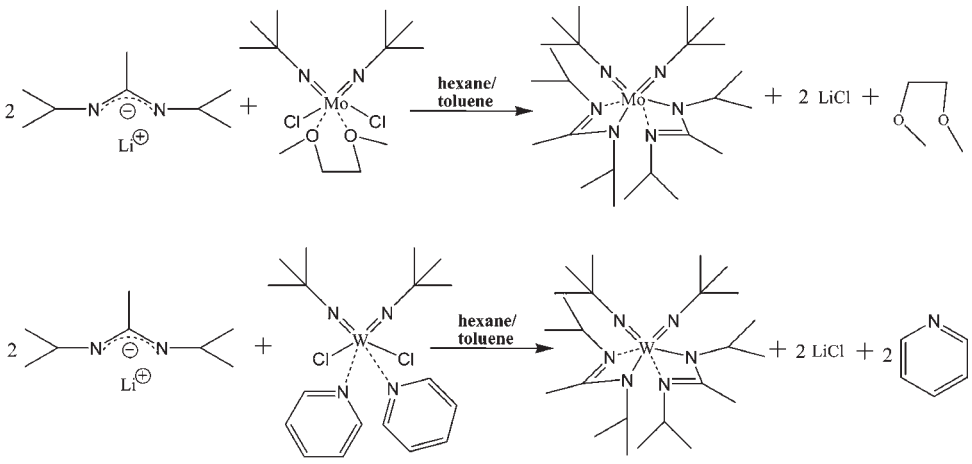

pressure of 8×10^{-6} mbar to remove any gaseous impurities. Prior to film growth, the Si(100) substrates (1 cm × 1 cm) were ultrasonically cleaned in acetone, isopropyl alcohol, and deionized water, subsequently rinsed with deionized water (Millipore Water Purification System), and dried under an argon gas stream. Film deposition was carried out in a temperature range of 500−800 °C, and the susceptor temperature was varied in steps of 100 °C. During deposition, the reactor pressure was maintained at 1 mbar. For each deposition, about 50 mg of compound (**1**) was used and the precursor was vaporized at 130 °C using nitrogen as the carrier gas (50 sccm, 99.9999%). Ammonia (50 sccm, 99.998%) was used as the reactive gas. The gas flow rates were monitored using mass flow controllers (MKS Instruments).

[Mo(N*t*Bu)$_2${(*i*PrN)$_2$CMe}$_2$] (1). A 1.6 M solution of methyllithium in diethyl ether (19.5 mL, 0.0312 mol) was added in the cold to a mixture of *N*,*N*′-diisopropylcarbodiimide (4.9 mL, 0.0312 mol) in hexane (30 mL). The solution was stirred for approximately 2 h until precipitation of the lithium amidinate salt was complete. To this suspension was added [Mo(N*t*Bu)$_2$Cl$_2$(dme)] (6.22 g, 0.0156 mol) dissolved in toluene (40 mL). After stirring for 12 h at ambient conditions, the solvent was removed by filtration (Celite). The orange solid left behind was recrystallized in toluene/hexane, yielding 3.1 g (37.6%), and then further purified by sublimation at 130 °C (1 mTorr).

^{1}H NMR (298 K, 250 MHz, C_6D_6): δ_H 1.15 (d, 6H, N*i*Pr), 1.24 (d, 6H, N*i*Pr), 1.35 (d, 6H, N*i*Pr), 1.40 (d, 6H, N*i*Pr), 1.49 (s, 18H, N*t*Bu), 1.55 (s, 6H, (*i*PrN)$_2$C*Me*), 3.65 (sept, 2H, N*i*Pr), 3.78 (sept, 2H, N*i*Pr).

^{13}C NMR (298 K, 250 MHz, C_6D_6): δ_C 11.12 ((N*i*Pr)$_2$C*Me*), 23.49 (NCH*Me*$_2$), 25.90 (NCH*Me*$_2$), 26.17 ((NCH*Me*$_2$), 26.69 (NCH*Me*$_2$), 32.17 (NC*Me*$_3$), 48.03 (Me$_2$*C*HN), 48.35 (Me$_2$*C*HN), 67.89 (N*C*Me$_3$), 167.67 (*C*N$_2$).

Elem anal. Calcd for $C_{24}H_{52}N_6Mo$: C, 55.36; H, 10.07; N, 16.14. Found: C, 55.38; H, 10.04; N, 16.40.

FTIR (solid): 1106, s (ν_{M-NR}, δ_{tBu}); 1202, vs (ν_{MN-R}, δ_{C-H}), 1559, s ($\nu_{as\ M-N-C}$, $\nu_{as\ N-C-N}$); 2961, s ($\nu_{as\ CH_3}$).

EI-MS [*m*/*z* (%)]: 522 (1) $[M]^{\bullet+}$; 507 (4) $[M - CH_3]^+$; 465 (0.5) $[M - CH_3 - C_3H_6]^+$; 451 (4) $[M - CH_3 - C_4H_8]^+$; 141 (100) $[N_2C_8H_{14}]^{\bullet+}$; 56 (2) $[C_4H_8]^{\bullet+}$; 42 (55) $[C_3H_6]^{\bullet+}$.

[W(N*t*Bu)$_2${(*i*PrN)$_2$CMe}$_2$] (2). This compound was synthesized in a manner similar to that described for **1**. Instead of [Mo(N*t*Bu)$_2$Cl$_2$(dme)], [WCl$_2$(N*t*Bu)$_2$py$_2$] (11 g, 19.8 mmol) was used. The product was isolated as a brown solid. Yield: 6.2 g (51.4%) after recrystallization in hexane/toluene. Sublimation at 130 °C (1 mTorr) gave a bright-yellow compound.

^{1}H NMR (298 K, 250 MHz, C_6D_6): δ_H 1.08 (d, 6H, N*i*Pr), 1.29 (d, 6H, N*i*Pr), 1.33 (d, 6H, N*i*Pr), 1.41 (d, 6H, N*i*Pr), 1.47 (s, 6H, (*i*PrN)$_2$C*Me*), 1.52 (s, 18H, N*t*Bu), 3.65 (sept, 2H, N*i*Pr), 3.96 (sept, 2H, N*i*Pr).

^{13}C NMR (298 K, 250 MHz, C_6D_6): δ_C 11.80 ((N*i*Pr)$_2$C*Me*), 23.26 (NCH*Me*$_2$), 25.58 (NCH*Me*$_2$), 26.05 ((NCH*Me*$_2$), 26.72 (NCH*Me*$_2$), 33.57 (NC*Me*$_3$), 47.78 (Me$_2$*C*HN), 47.84 (Me$_2$-*C*HN), 48.78 (Me$_2$*C*HN), 66.04 (N*C*Me$_3$), 167.57 (*C*N$_2$).

UV/vis (toluene): λ_{max} 295 nm. Elem anal. Calcd for $C_{24}H_{52}N_6W$: C, 47.37; H, 8.61; N, 13.81. Found: C, 46.78; H, 8.71; N, 14.03.

FTIR (solid): 1131, s (ν_{M-NR}, δ_{tBu}); 1205, vs (ν_{MN-R}, δ_{C-H}); 1557, s ($\nu_{as\ M-N-C}$, $\nu_{as\ N-C-N}$); 2959, s ($\nu_{as\ CH_3}$).

EI-MS [*m*/*z* (%)]: 608 (4) $[M]^{\bullet+}$; 593 (58) $[M - CH_3]^+$; 551 (1) $[M - CH_3 - C_3H_6]^+$; 537 (2) $[M - CH_3 - C_4H_8]^+$; 468 (13) $[M - N_2C_8H_{16}]^{\bullet+}$; 141 (16) $[N_2C_8H_{14}]^{\bullet+}$; 56 (2) $[C_4H_8]^{\bullet+}$; 42 (100) $[C_3H_6]^{\bullet+}$.

Results and Discussion

Synthesis. The amidinato/imido complexes **1** and **2** were synthesized by reacting the amidinate salt, which was obtained *in situ* by treating *N*,*N*′-diisopropylcarbodiimide with methyllithium, with the appropriate metal imido precursor [Mo(N*t*Bu)$_2$Cl$_2$(dme)] or [WCl$_2$(N*t*Bu)$_2$(py)] (Scheme 1). The yields of 40−60% pure compound after recrystallization were acceptable. Unfortunately, single crystals suitable for structural characterization by X-ray diffraction (XRD) could not be obtained. The molecules were continuously disordered irrespective of the crystallization conditions. This problem may be solved by variation of the substitution pattern; however, we rather decided to perform DFT calculations to derive structural data for comparison in order to support our spectroscopic and mass-spectrometric characterization given below.

Structural Characterization Based on DFT Calculations. Because of the highly disordered single crystals, *ab initio* DFT calculations for geometry optimization have been performed on **2** (Figure 1). The overall structural features of the Mo congener **1** should be quite similar. The tungsten atom of **2** is surrounded by a distorted octahedron of nitrogen atoms. The *cis* arrangement of each of the two types of ligands turned out to be the only accessible isomer in the calculations; all efforts to find a stable *trans* structure were not successful.

We focus our discussion on an analysis of the bonding properties of the imido ligands (Scheme 2). Imido ligands may exhibit a linear arrangement and a double bond with one free electron pair located at nitrogen(I), a linear triply bonded

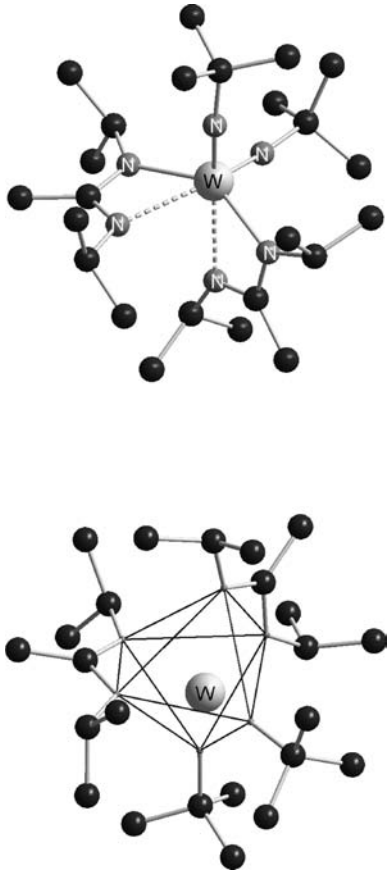

Figure 1. (Top) Calculated structure **2**. (Bottom) Coordination polyhedron of the nitrogen atoms around the tungsten atom in the form of a distorted octahedron, indicating *cis* isomerism.

Scheme 2. Different Possible Arrangements of the Imido and Amidinato Groups

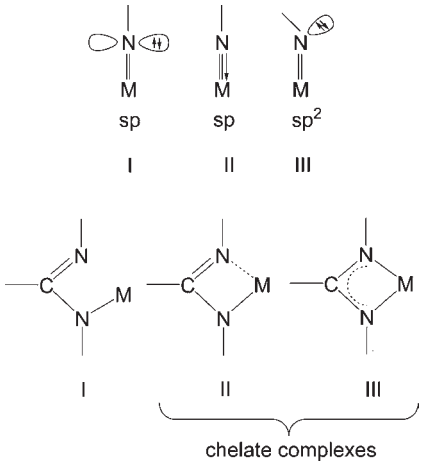

nitrogen(II), or a bent geometry for nitrogen(III).[27,28] Linear structures have M−N−C angles between 180 and 160°, a "semibent" structure is present between 160 and 150°, and the imido ligand is bent with a stereochemically active lone pair at the nitrogen atom between 150 and 130°.[27a] Linear imido ligands are considered as formally four-electron donors in contrast to bent imido ligands being only formally two-electron donors[27] just as imido groups acting as three-electron donors have been reported.[27] In the calculated structure of **2**, the W−N bond lengths are 181 and 181.5 pm and the W−N−C angles 166.2 and 168°. In order to validate the quality of the DFT calculations on **2** and to define differences between the obtained theoretical structure and experimental values, the related molecule $[WCl_3(N\textit{i}Pr)\{(\textit{i}PrN)_2C(NMe)_2\}]$[22b] was also calculated and compared with its experimentally determined structure. As a result, the calculated W−N*t*Bu bonds were about 7 ppm longer than the experimental values, in contrast to the W−N−C angles being 10° more acute in the experimentally determined structure than in the calculated one. Taking these deviations into account for assignment of the calculated structure of **2** to one of the limiting cases above leads to an estimation of decreased bond lengths around 174 pm in the actual structure, which, however, are, nevertheless, clearly in the upper range of a W−N triple bond (ca. 164−174 pm),[29] whereas the W−N−C angles decreased as well down to approximately 157°, being at the threshold of the linear and "semibent" area. Certainly, this reasoning provides only a rough estimation of the differences between theory and experiment including deviations from packing effects in the crystal structure as well as thermal contributions (in DFT calculations, the isolated molecule is assumed to be at its ground state at $T = 0$ K) and, of course, DFT calculations imply a systematic lack of accuracy.[30]

Relating to experimentally achieved results, most characterized early-transition-metal alkylimido complexes have M−N−R angles > 160°.[31] Surprisingly, in the range 160−180°, no correlation can be drawn between the bond order and angle.[32] Concerning bond orders, transition-metal imido complexes are not restricted to either double or triple bonds. The true bonding situation may lie between both extremes,[27b,28,29,33] being a very likely case for the bonding situation in the tungsten complex **2**. Because of symmetry restrictions, the number of electrons that can be donated to the metal is reduced to six for two imido ligands in a *cis*-octahedral complex.[33] Therefore, each imido group acts as a formal three-electron donor, resulting in an 18-electron complex. In addition, the amidinato W−N bonds *trans* to the imido groups show an increased distance due to the thermodynamic *trans* influence.

NMR Spectroscopy. The ^{1}H and ^{13}C NMR spectra of **1** and **2** are given in Figure 2 and reveal the expected signals. The experimentally obtained ^{13}C values are in good agreement with the calculated ones (see the Supporting Information). A matter of particular interest here are the different ^{1}H chemical shifts of the isopropyl doublets, providing some information about the atomic arrangement. Diverse bonding modes of amidinato complexes

(27) (a) Barrie, P.; Coffey, T. A.; Forster, G. D.; Hogarth, G. *J. Chem. Soc., Dalton Trans.* **1999**, 4519–4528. (b) Cundari, T. R. *Chem. Rev.* **2000**, *100*, 807–818.
(28) Parkin, G.; van Asselt, A.; Leahy, D. J.; Whinnery, L.; Hua, N. G.; Quan, R. W.; Henling, L. M.; Schaefer, W. P.; Santarsiero, B. D.; Bercaw, J. E. *Inorg. Chem.* **1992**, *31*, 82–85.
(29) Radius, U.; Sundermeyer, J.; Pritzkow, H. *Chem. Ber.* **1994**, *127*, 1827–1835.
(30) Hoffmann, R.; von Ragué Schleyer, P.; Schaefer, H. F., III *Angew. Chem., Int. Ed.* **2008**, *47*, 7164–7167.
(31) (a) Cundari, T. R. *J. Am. Chem. Soc.* **1992**, *114*, 7879–7888. (b) Nugent, W. A.; Mayer, J. M. *Metal−Ligand Multiple Bonds*; Wiley: New York, 1989.
(32) Schorm, A.; Sundermeyer, J. *Eur. J. Inorg. Chem.* **2001**, 2947–2955.
(33) Nugent, W. A.; Haymore, B. L. *Coord. Chem. Rev.* **1980**, *31*, 123–175.

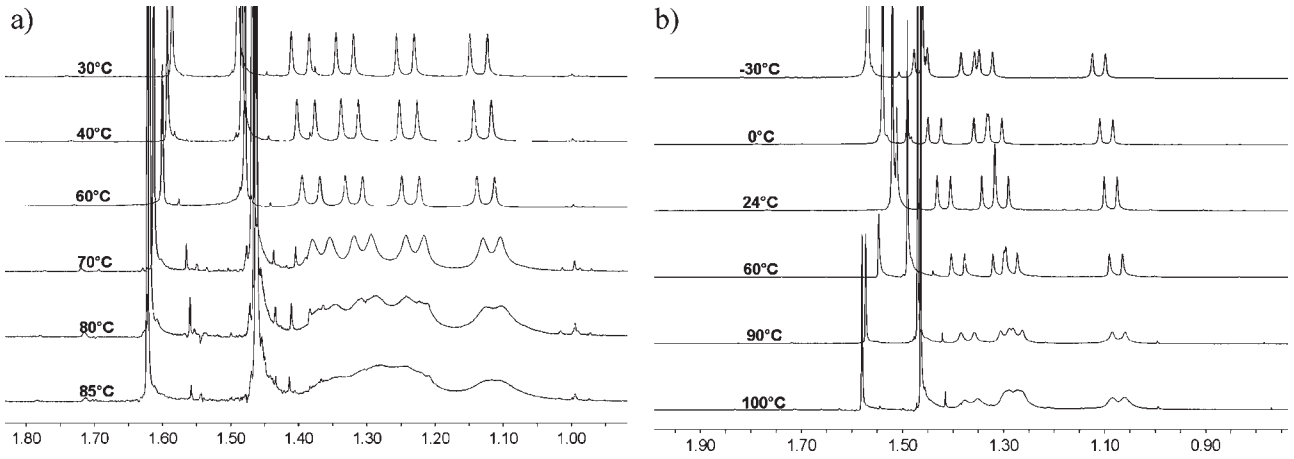

Figure 2. Temperature-dependent ^{1}H NMR spectra of (a) complex **1** and (b) complex **2** in toluene-d_8.

have been described (Scheme 2).[34] In the monodentate amidinato form (I), one nitrogen is σ-bonded to the metal, whereas the other reveals no interactions. The chelate bonding mode can be unsymmetric (II) or symmetric (III). By a comparison of the crystal structures and the appropriate ^{1}H NMR spectra of published *N*-isopropyl-substituted amidinato ligands, the following conclusions can be drawn: As to highly symmetric structures with a difference of less than 1.4 ppm between the two amidinate M−N σ bonds and N−C bond lengths between 129 pm (C=N double bond) and 147 pm (C−N single bond),[35] a single doublet representing two (or four) isopropyl groups appears in the ^{1}H NMR spectra.[36] As exceptions of this trend, the germanium [Ge{(*i*PrN)$_2$CMe}$_2$][37] and the aluminum bis(amidinato) complex [Al{(*i*PrN)$_2$CMe}$_2$]Cl[36a] reveal only a single doublet in the ^{1}H NMR spectra, while the single-crystal structure indicates a comparably large difference between the respective M−N bond lengths of 31.8 pm each (germanium complex) and 12.7 pm each (aluminum complex). The differences in the C−N bond lengths are 2.3 pm (germanium complex) and 1.8 pm (aluminum complex). In this case, the solid-state structure seems to be highly different from the symmetric geometry present in solution, where free rotation about the M−N axis because of low sterical hindrance is possible. In summary, differences in the C−N bond lengths in the single-crystal structure greater than 1.8 pm as well as differences between the M−N bond lengths greater than 5 pm suggest an unsymmetrically bonded chelate complex present in solution, leading to separated isopropyl signals in the NMR spectrum.[36e,37,38] Note that *N*,*N*′-diisopropyl[2,6-bis(mesityl)]benzamidine[36c] can be considered as an example of a rare monodentate amidinato complex with M−N and C−N differences of 132.7 and 5.2 pm, respectively.

Turning now the attention back to the NMR data of the amidinato/imido complexes **1** and **2** (Figure 2), the unequal ^{1}H chemical shifts for each isoproyl group clearly suggest an unsymetrically bonding mode, whose assignment nicely matches the calculated structure of **2**. Because of the fact that deshielding of the quarternary *tert*-butyl carbon atom is closely related to the metal Lewis acidity,[39] ^{13}C NMR shifts enable a comparison of **1** and **2** in this regard. The difference $\Delta\delta$ between the chemical shifts of the primary carbon atoms and the quaternary one reflects the degree of electron density at the metal. The resulting values for **1** ($\Delta\delta$ = 35.72) and **2** ($\Delta\delta$ = 32.47) manifest for these amidinato/imido compounds a greater Lewis acidity at the molybdenum atom compared to the tungsten atom. Comparable trends with a molybdenum complex representing a more acidic center than its tungsten congener were already published.[39a] To examine the fluxional behavior, temperature-dependent NMR spectra have been recorded. As expected by unsymmetrical coordination, coalescence of only two doublets is observed because of rotation about the shortest M−N axis of each amidinato ligand. The obtained data enable determination of the rate constant at the coalescence temperature k_C as well as the Gibbs energy of activation $\Delta G^{\ddagger}_C$ for rotation about the M−N bond (Table 2).[40]

Mass Spectrometry. EI-MS spectra were recorded for **1** and **2** (Table 3). In either spectra, the molecular ion peak was detected, indicating evaporation of the intact molecule under the conditions of the measurement. The molecular ion as well as the assigned fragments each reflect the isotopic distribution of the metals (see the Supporting Information). The prominent fragmentation occurring in both cases was loss of a CH_3 radical. This process occurs at α-heteroatom bonds (α cleavage). Presumably, the amidinato C−methyl group will split preferably because

(34) (a) Barker, J.; Kilner, M. *Coord. Chem. Rev.* **1994**, *133*, 219–300. (b) Kissounko, D. A.; Zabalov, M. V.; Brusova, G. P.; Lemenovskii, D. A. *Russ. Chem. Rev.* **2006**, *75*(5), 351–374.

(35) Müller, P., Ed. *Crystal Structure Refinement—A Crystallographer's Guide to SHELXL*; Oxford University Press: Oxford, U.K., 2007.

(36) (a) Coles, M. P.; Swenson, D. C.; Jordan, R. F.; Young, V. G., Jr. *Organometallics* **1997**, *16*, 5183–5194. (b) Schmidt, J. A. R.; Arnold, J. *J. Chem. Soc., Dalton Trans.* **2002**, 3454–3461. (c) Schmidt, J. A. R.; Arnold, J. *J. Chem. Soc., Dalton Trans.* **2002**, 2890–2899. (d) Bambirra, S.; Brandsma, M. J. R.; Brussee, E. A. C.; Meetsma, A.; Hessen, B.; Teuben, J. H. *Organometallics* **2000**, *19*, 3197–3204. (e) Decker, J. M.; Geib, S. J.; Meyer, T. Y. *Organometallics* **1999**, *18*, 4417–4420.

(37) Karsch, H. H.; Schlüter, P. A.; Reisky, M. *Eur. J. Inorg. Chem.* **1998**, 433–436.

(38) Vendemiati, B.; Prini, G.; Meetsma, A.; Hessen, B.; Teuben, J. H.; Traverso, O. *Eur. J. Inorg. Chem.* **2001**, 707–711.

(39) (a) Sundermeyer, J. *Chem. Ber.* **1991**, *124*, 1977–1979. (b) Nugent, W. A.; McKinney, R. J.; Kasovsky, R. V.; Van-Catledge, F. A. *Inorg. Chim. Acta* **1982**, *65*, L91–L93.

(40) Calculations were performed using standard formulas: $k_C = 2.22\Delta\nu$, where $\Delta\nu$ was obtained by measuring the ^{1}H NMR spectra at 213 K; $\Delta G^{\ddagger}_C = 19.14T_C[10.32 + \log(T_C/k_C)]$. See: Friebolin, H. *Ein- und zweidimensionale NMR-Spektroskopie*; Wiley-VCH: Weinheim, Germany, 2006.

Table 2. Parameters Obtained by Dynamic NMR Spectroscopy

compound	$\Delta\nu$(213 K) (Hz)	k_C (s^{-1})	$\Delta G^{\ddagger}_C$ (kJ/mol)
1	32.5	$k_{358} = 72$	$\Delta G^{\ddagger}_{358} = 75.5 \pm 0.9$
2	147	$k_{373} = 326$	$\Delta G^{\ddagger}_{373} = 74.1 \pm 1.0$

Table 3. Abundances for EI-MS Spectra for Tungsten and Molybdenum Complexes **1** and **2** Recorded by Normalization of the Base Peak Intensity to 100% Relative Intensity

	Mo complex		W complex	
fragments	*m*/*z*	relative intensity (%)	*m*/*z*	relative intensity (%)
$M^{\bullet+}$	522	1	608	4
$[M - CH_3]^+$	507	4	593	58
$[M - CH_3 - C_3H_6]^+$	465	0.5	551	1
$[M - CH_3 - C_4H_8]^+$	451	4	537	2
$[W - N_2C_8H_{16}]^{\bullet+}$			468	13
$[N_2C_8H_{14}]^{\bullet+}$	141	100	141	16
$[C_4H_8]^{\bullet+}$	56	2	56	2
$[C_3H_6]^{\bullet+}$	42	55	42	100

of its two adjacent nitrogen atoms. The demethylated fragments of **1** and **2** give rise to further onium reactions, resulting in a loss of either propene (being the base peak in the spectra of **2**) or isobutene, already mentioned for tungsten imido complexes [WCl_4(N*i*Pr)] and [$WCl_4(NC_3H_5)$].[41] Just as well as an onium reaction might occur, a McLafferty rearrangement by splitting off propene is also probable. In the case of **2**, a fragmentation caused via β-hydrogen migration is assumed. On the basis of computational studies, this decomposition process was proposed for molybdenum amido/imido compounds.[42] In summary, the fragmentation process always occurs, retaining a six-valence metal ion. The obtained fragmentation scheme is consistent with the nitrogen rule[43] and the rings plus double bonds equation.[44] Although ionization by electron impact is not comparable with the thermal processes taking place in a CVD reactor, related mechanistic steps have been proposed for interpretation of the deposited layers.[41,45] High-resolution measurements have been performed, revealing deviations between the calculated exact mass and the experimentally accurate mass well within the accepted error range of ±5 mmu (Table 1).[44] Therefore, the elemental compositions are confirmed. Additionally, high-resolution mass spectrometry supports selected fragments of Scheme 3 (see the Supporting Information).

IR Spectroscopy. The IR spectra show some prominent peaks, which were assigned with the help of literature data (Figure 3 and Table 4). Concerning metal *tert*-butylimido vibrational frequencies, actual research has been released including a comparison of measured IR data with calculated values and determination of the Raman features with isotope labeling.[46] On the other hand, only one IR band assignment of a single metal amidinato complex could be found in the literature.[47] Additionally, spectra of

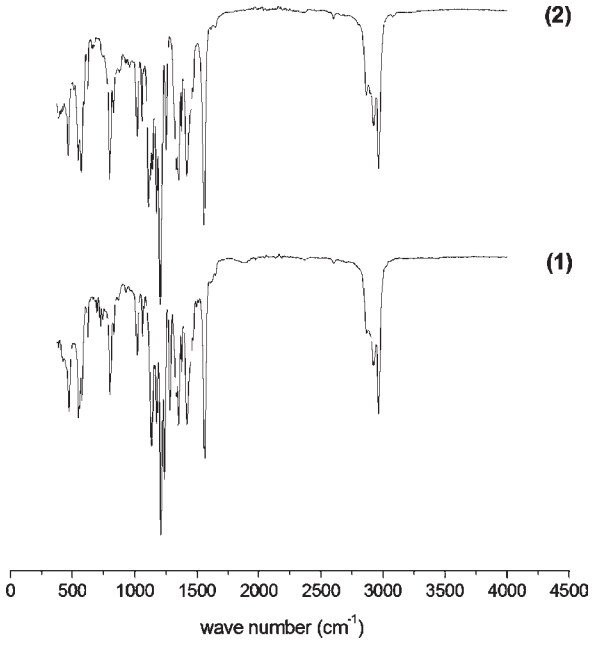

Figure 3. FTIR spectra of **1** (bottom) and **2** (top).

Scheme 3. Proposed EI-MS Fragmentation Scheme for Compounds **1** and **2**

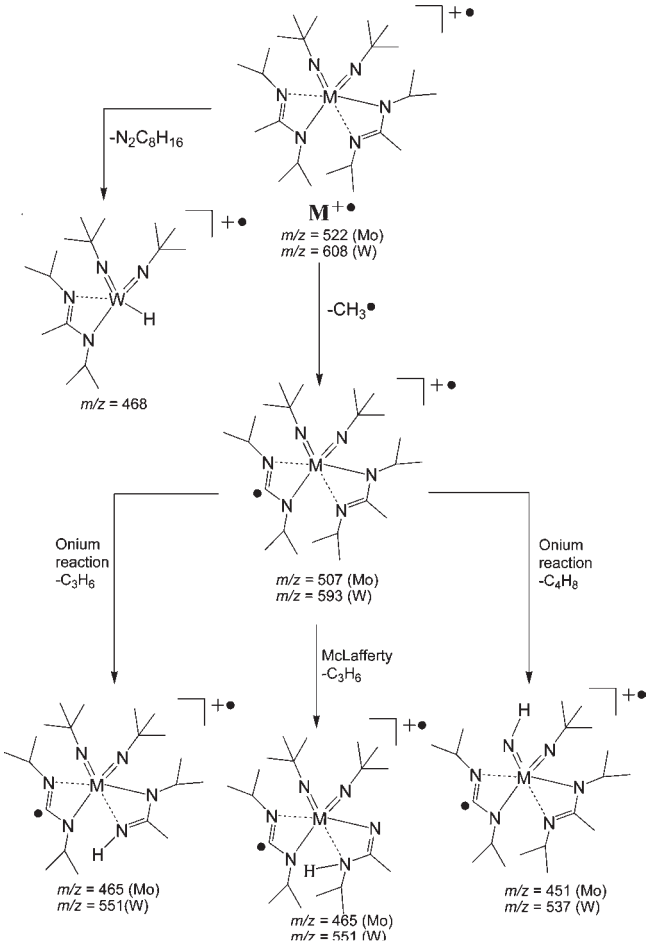

(41) Won, Y. S.; Kim, Y. S.; Anderson, T. J.; McElwee-White, L. *Chem. Mater.* **2008**, *20*, 7246–7251.
(42) Miikkulainen, V.; Suvanto, M.; Pakkanen, T. A. *Chem. Vap. Deposition* **2008**, *14*, 71–77.
(43) Watson, J. T.; Sparkman, O. D. *Introduction to Mass Spectrometry*; Wiley: New York, 2009.
(44) Gross, J. H. *Mass Spectrometry*; Springer: Berlin, 2004.
(45) (a) Bchir, O. J.; Green, K. M.; Ajmera, H. M.; Zapp, E. A.; Anderson, T. J.; Brooks, B. C.; Reitfort, L. L.; Powell, D. H.; Abboud, K. A.; McElwee-White, L. *J. Am. Chem. Soc.* **2005**, *127*, 7825–7833. (b) Milanov, A. P.; Thiede, T. B.; Devi, A.; Fischer, R. A. *J. Am. Chem. Soc.* **2009**, *131*, 17062–17063.

Table 4. Assignment of Characteristic FTIR Frequencies in the Solid State

	ν_{M-NR}, δ_{tBu} (cm^{-1})	ν_{MN-R}, δ_{C-H} (cm^{-1})	$\nu_{as\ M-N-C}$, $\nu_{as\ N-C-N}$ (cm^{-1})	$\nu_{as\ CH_3}$ (cm^{-1})
1	1106	1202	1559	2961
2	1131	1205	1557	2959

amidines[48] and bridged amidinato complexes (i.e., complexes involving a M_2NCN ring)[49] offer clues for interpretation of the IR bands originating from amidinato ligands. Another aspect that complicates assignment of the IR peaks is the vibrational coupling of (CN), (CC), and (MN) modes, leading to complex absorption bands.

Amidinato M−N bonds: M−N single bonds can be observed from 200 to 850 cm^{-1} (as it has been shown for inorganic amides).[50] In the observed IR absorptions, the M−N vibration modes could not be assigned, probably lying out of range of the measured spectra. Amidinato C−N and C−C bonds: The single metal amidinato complex [Rh(η-C_5Me_5)Cl{(p-$MeC_6H_4N)_2CH$}][47] as well as bridged amidinato complexes[49] show IR absorption bands around 1560 cm^{-1} assignable to the asymmetric (N−C−N) stretching mode. As to amidine IR bands, differentiations between C−N single and double bonds have been made.[48] Nevertheless, a considerable double-bond character was also claimed for the C−N single bond. Absorptions around 1250 cm^{-1} were related to an increased double-bond character of the C−N vibration, whereas the C═N double bonds in N-disubstituted trichloroacetamidines give rise to absorption bands at ∼1560 cm^{-1}. Imido M−N bonds: Three main stretching modes for tantalum alkylimido compounds have been calculated: ν_s(M−N−C) at ∼630 cm^{-1}, ν_sM−(N−C) at ∼1280 cm^{-1}, and ν_{as}(M−N−C) at ∼1560 cm^{-1}. However, only the latter ones were observable in the spectra.[46a] The stretching mode at 1100 cm^{-1} is assigned to be primarily composed of a M−N vibration; to a lesser extent, it is attributed to *tert*-butyl deformations.[46b] Additionally, some weak metal−ligand deformation modes are assumed to be below 500 cm^{-1}. Imido C−N and C−H bonds: As per Korolev et al., the mode at ∼1280 cm^{-1} owns mainly CN and CH character, and the vibrations at higher frequencies (∼1580 cm^{-1}) originate from nitrogen motions along the M−N−C axis.[46a] Mehn et al.[46b] assign the mode primarily composed of CN features at ∼1235 cm^{-1}.

Thus, assignment of the observed IR bands for **1** and **2** is as follows: The strong absorption bands at 1106 cm^{-1} (**1**) and 1133 cm^{-1} (**2**) are attributed to the imido M−N stretching mode according to the conclusions of Mehn et al.[46b] As to Dehnicke and Strähle, the M−N wavenumber of structurally comparable species increases down a group caused by an increased ability to effect π overlap.[51]

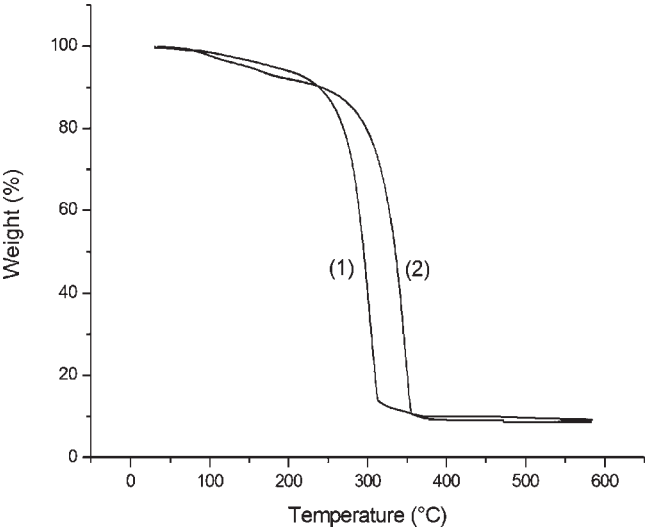

Figure 4. TGA of **1** and **2**.

This trend can be confirmed here. Values near 1200 cm^{-1} originate from C−N stretching frequencies;[46,48,52] presumably, *tert*-butyl deformation modes[46b] contribute to this very strong band in the IR spectra of the molybdenum and tungsten compounds. The region around 1560 cm^{-1} seems to indicate CN vibration modes as well, including some metal character.[46a,47−49] At ∼2960 cm^{-1}, asymmetric stretching vibrations of methyl groups appear.[53] In summary, the vibration ∼1100 cm^{-1} can be assigned quite probably mainly to the M−imido−N stretching frequencies. Other vibrational modes cannot be clearly attributed to either the amidinato or imido ligand.

Thermal Properties. Sublimation of 1.5 g of **2** at 130 °C and 1 mTorr yields 1 g (66%) of the purified tungsten complex. Examining the thermal properties of the compounds by thermogravimetric analysis (TGA) at a linear temperature ramp of 5 °C/min reveals an almost single step mass loss starting at 250 °C for **1** and 300 °C for **2** both within a temperature window of 50 °C (Figure 4). As deduced from the comparably low residual mass of about 10 wt %, sublimation and decomposition are coupled at the temperature window of 250−350 °C because the residual masses expected for a quantitative conversion of **1** and **2** to the respective MN_x or other multinary $M(N,C,H)_y$ materials are around 20 wt % (Mo) or 30 wt % (W). Interestingly, above 100 °C and up to the onset of decomposition, a continuous mass loss of approximately 10 wt % is observable.

Preliminary MOCVD Experiments. To evaluate the performance of **1** as a potential precursor for MOCVD of molybdenum nitride thin films, preliminary film deposition experiments were conducted. The details of the deposition procedure are described in the experimental part. Molybdenum nitride films were grown at substrate temperatures between 500 and 800 °C on Si(100) substrates using compound **1** in combination with ammonia. The obtained films were silver−golden in color and showed a metallic luster. XRD analysis revealed the

(46) (a) Korolev, A. V.; Rheingold, A. L.; Williams, D. S. *Inorg. Chem.* **1997**, *36*, 2647–2655. (b) Mehn, M. P.; Brown, S. D.; Jenkins, D. M.; Peters, J. C.; Que, L., Jr. *Inorg. Chem.* **2006**, *45*, 7417–7427.
(47) Piraino, P.; Bruno, G.; Tresoldi, G.; Faraone, G.; Bombieri, G. *J. Chem. Soc., Dalton Trans.* **1983**, *11*, 2391–2395.
(48) Grivas, J. C.; Taurins, A. *Can. J. Chem.* **1959**, *37*, 795–802.
(49) (a) Piraino, P.; Bruno, G.; Tresoldi, G.; Lo Schiavo, S.; Nicolò, F. *Inorg. Chem.* **1989**, *28*, 139–144. (b) Rotondo, E.; Bruno, G.; Nicolò, F.; Lo Schiavo, S.; Piraino, P. *Inorg. Chem.* **1991**, *30*, 1195–1200.
(50) Lucazeau, G.; Guemas, L.; Novak, A. *Inorg. Chim. Acta* **1976**, *20*, 11–18.
(51) Dehnicke, K.; Strähle, J. *Angew. Chem., Int. Ed.* **1981**, *20*, 413–426.
(52) Glueck, D. S.; Hollander, F. J.; Bergman, R. G. *J. Am. Chem. Soc.* **1989**, *111*, 2719–2721.
(53) Gottwald, W.; Wachter, G. *IR-Spektroskopie für Anwender*; Wiley-VCH: Weinheim, Germany, 1997.

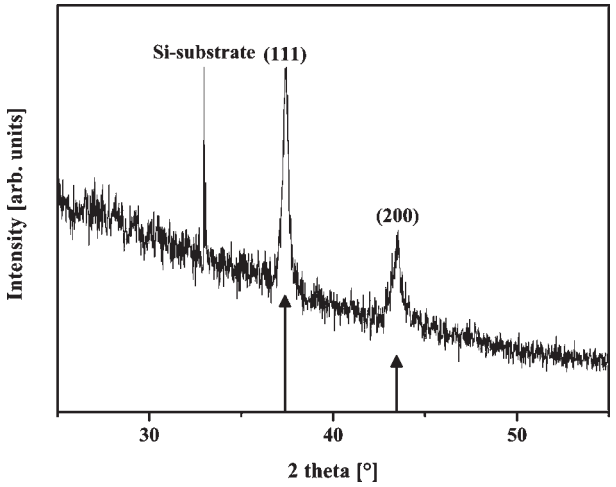

Figure 5. XRD analysis of a molybdenum nitride film deposited at 800 °C. The vertical lines with a triangle on top display the positions of the (111) and (200) reflections of γ-Mo_2N (JC-PDF 00-025-1366).

nanocrystalline/amorphous nature of films deposited at 500 °C, indicated by the presence of broad reflections with low intensity (Figure 5). At higher substrate temperatures, clear reflexes corresponding to the (111) and (200) reflections of γ-Mo_2N (JC-PDF 00-025-1366) were observed, indicating that the crystalline part of the deposited film consists of the γ phase of molybdenum nitride. The peak at around 33° arises from the silicon substrate.

Conclusions

The two compounds **1** and **2** are the first examples of all-nitrogen coordinated bis(alkylamidinato)/bis(alkylimido) complexes of molybdenum and tungsten. DFT calculations on **2** confirm the preference of the *cis* isomer and allow deduction of a bond order of the *tert*-butylimido group between two and three. Both DFT calculations and the NMR data support assignment of the unsymmetrically coordinated amidinato ligands. The elemental composition and parts of the fragmentation pattern under the conditions of electron impact ionization are unambiguously confirmed by high-resolution mass spectrometry. The thermal properties of both compounds are promising and allow for application as a MOCVD and ALD precursor, and variation of the substitution patterns of the alkyl groups is likely to allow tuning of the thermal properties to some extent. Preliminary investigations on the use of compound **1** for MOCVD applications in the presence of ammonia revealed the formation of molybdenum nitride thin films on silicon substrates.

Acknowledgment. This work has been supported by the Research Department "Integrity of Small-Scale Systems/High-Temperature Materials" (IS3/HTM) of the Ruhr University Bochum (http://www.rd.ruhr-uni-bochum.de/is3/index.html).

Supporting Information Available: Table of calculated ^{13}C NMR shifts for **2**, mass spectra of **1** and **2**, and a table with high-resolution mass spectrometry data. This material is available free of charge via the Internet at http://pubs.acs.org.